

T h e P h a n t o m L a b o r a t o r y

## C a t p h a n<sup>®</sup> 605 Product Guide

Copyright © 2021

### WARRANTY

THE PHANTOM LABORATORY INCORPORATED (“Seller”) warrants that this product shall remain in good working order and free of all material defects for a period of one (1) year following the date of purchase. If, prior to the expiration of the one (1) year warranty period, the product becomes defective, Buyer shall return the product to the Seller at:

By Truck

The Phantom Laboratory, Incorporated  
2727 State Route 29  
Greenwich, NY 12834

By Mail

The Phantom Laboratory, Incorporated  
PO Box 511  
Salem, NY 12865-0511

Seller shall, at Seller’s sole option, repair or replace the defective product. The Warranty does not cover damage to the product resulting from accident or misuse.

IF THE PRODUCT IS NOT IN GOOD WORKING ORDER AS WARRANTED, THE SOLE AND EXCLUSIVE REMEDY SHALL BE REPAIR OR REPLACEMENT, AT SELLER’S OPTION. IN NO EVENT SHALL SELLER BE LIABLE FOR ANY DAMAGES IN EXCESS OF THE PURCHASE PRICE OF THE PRODUCT. THIS LIMITATION APPLIES TO DAMAGES OF ANY KIND, INCLUDING, BUT NOT LIMITED TO, DIRECT OR INDIRECT DAMAGES, LOST PROFITS, OR OTHER SPECIAL, INCIDENTAL, OR CONSEQUENTIAL DAMAGES, WHETHER FOR BREACH OF CONTRACT, TORT OR OTHERWISE, OR WHETHER ARISING OUT OF THE USE OF OR INABILITY TO USE THE PRODUCT. ALL OTHER EXPRESS OR IMPLIED WARRANTIES, INCLUDING, BUT NOT LIMITED TO, THE IMPLIED WARRANTY OF MERCHANT ABILITY AND FITNESS FOR PARTICULAR PURPOSE, ARE HEREBY DISCLAIMED.

### WARNING

This product has an FH3-4 mm/min flame rating and is considered to be flammable. It is advised not to expose this product to open flame or high temperature (over 125° Celsius or 250° Fahrenheit) heating elements.

**CTP605**

**Medical device labeling**

Manufactured by: The Phantom Laboratory, Incorporated  
2727 State Route 29  
Greenwich, NY 12834 USA

EU Representative: Raförninn ehf  
Suðurhíð 35  
IS-105 Reykjavík ICELAND

Product: Catphan® 605

Model: CTP605

UDI:   
(01)00812266030383

Device Class: 1



This device is intended for use under direction of a trained medical physicist. Please refer to your machine manufacturer documentation and regulatory guidance for information on intended use.

A sample of this product has been assessed against the Essential Requirements of the EU Medical Device Regulation (MDR). The above mentioned product is deemed in compliance with MDR 2017/745 EU.

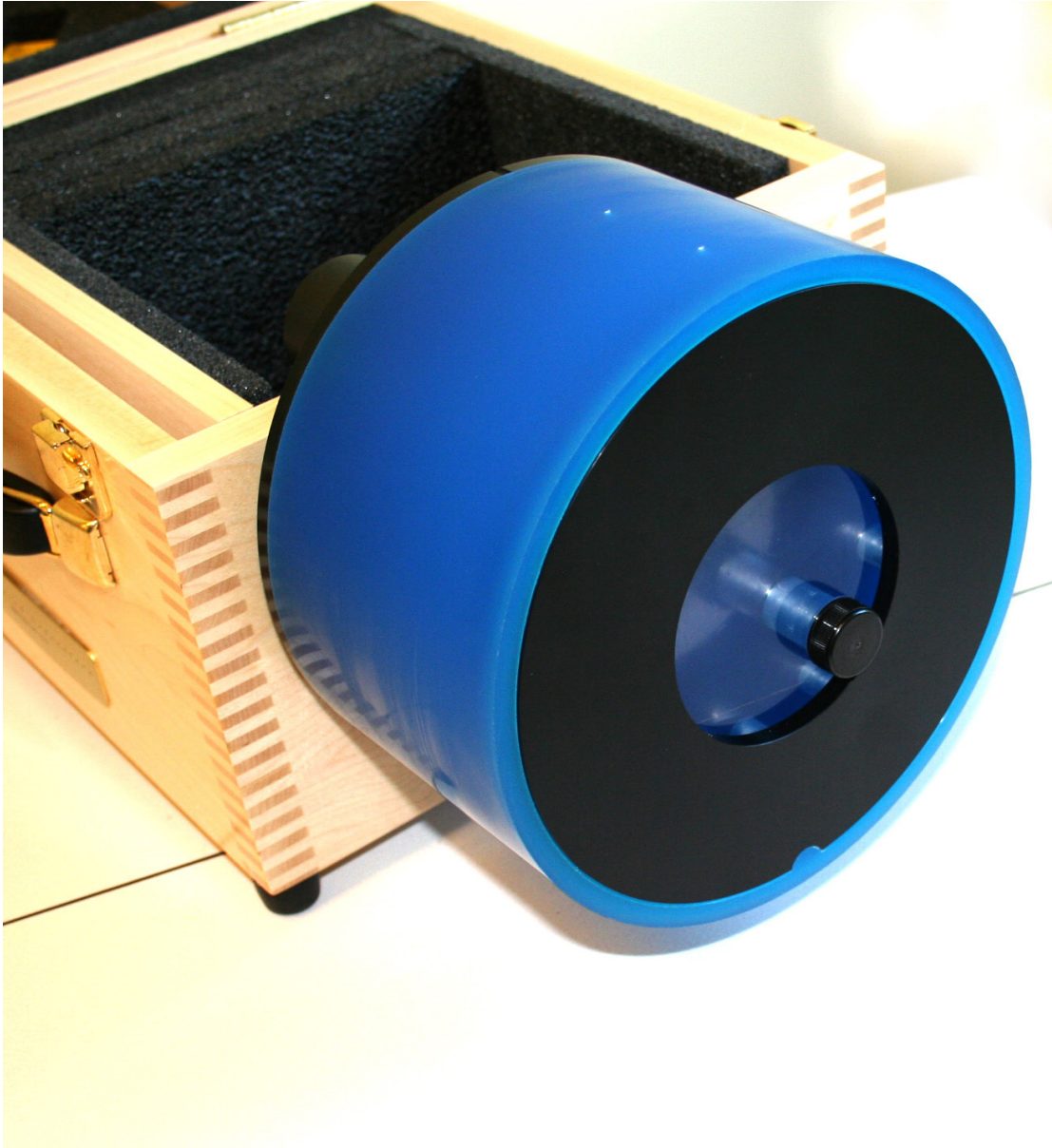
A risk assessment was conducted to the following standard: EN ISO14971  
This declaration of conformity is the result of testing and evaluation performed by The Phantom Laboratory, Incorporated.

# T h e P h a n t o m L a b o r a t o r y

## **Catphan® 605 Product Guide**

### *Contents*

Warranty	1
Introduction	5
Multi-Slice CT by David Goodenough, Ph.D.	6
Initial phantom positioning	8
Illustration of the Catphan® 605 module positions	9
Incremental phantom modules positioning	9
Phantom position verification	10
CTP682 Geometry, Sensitometry module	11
Scan slice geometry (slice width)	12
Slice width measurement with wire ramps	13
Scan incrementation	14
Slice width measurement with bead ramps	15
Measuring slice thickness with a profile made from bead image	17
Additional methods for estimating and measuring slice thickness with bead ramps	18
Patient alignment system check	19
Circular symmetry of display system	21
Spatial linearity and pixel size verification	21
Bead point source for point spread function and MTF	22
Use of automated scanner MTF programs	23
Bead point source for slice sensitivity profile	24
Spherical acrylic contrast targets	25
CT or Hounsfield Numbers by David Goodenough, Ph.D.	26
Sensitometry (CT number linearity)	27
Filling the water vial	28
CTP729 Image uniformity module	29
Automated computer analysis program	31
Optional phantom annuli	32
Dose Phantoms	33
Sample quality assurance program	34
Bibliography	35



**Catphan® 605**

## **Introduction**

The Phantom Laboratory and physicist, David J. Goodenough, Ph.D., are continually developing and researching new tests and modifications for the Catphan® phantoms. The test objects that make up the current Catphan® models embody more than a quarter century of scientific evaluation and field experience. This manual outlines the applications of each module contained in the Catphan® 605 phantoms.

We do not make specific recommendations on the content of your quality assurance program as each medical imaging facility has its own unique set of requirements. A sample program is provided to give you ideas for possible program content. We suggest a review of local governing regulations, manufacturers' specifications, and the needs of your radiologists and physicists before developing your CT quality assurance program.

If you have any additional questions please contact The Phantom Laboratory at:

Phone: 800-525-1190 or 518-692-1190

Fax: 518-692-3329

email: [sales@phantomlab.com](mailto:sales@phantomlab.com)

Additional product information is available at: [www.phantomlab.com](http://www.phantomlab.com)

## **Multi-Slice CT**

**by David J. Goodenough, Ph.D.**

At the request of The Phantom Laboratory I have put together this summary for physicists who are familiar with CT image performance measurements and have not had experience with multi-slice CT scanners.

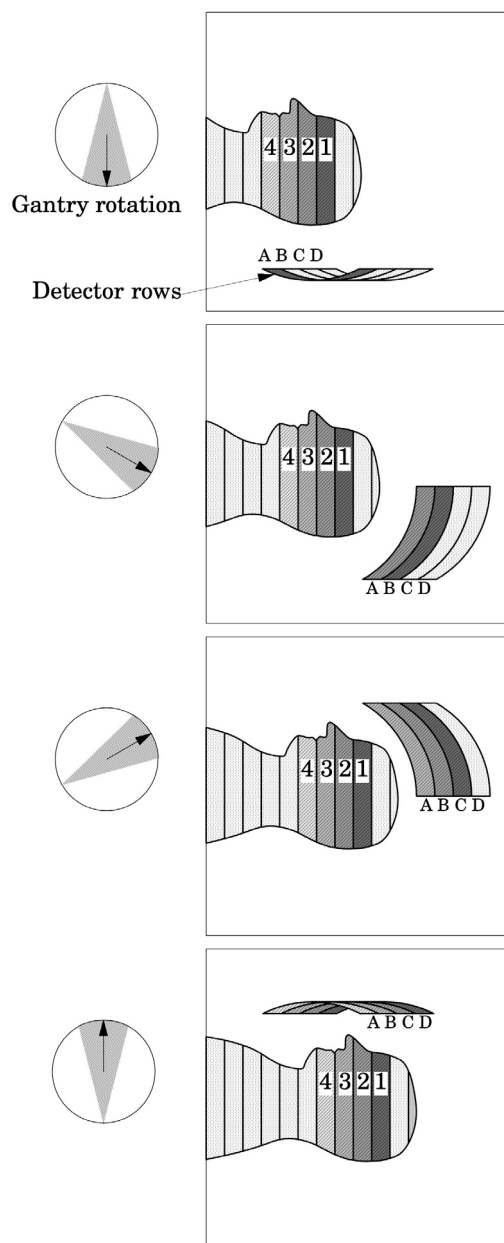
Multi-slice can use the same basic approach to image reconstruction as axial single slice CT. Each slice, or in some cases, the complete set of slices can be reconstructed from a “cone-beam” algorithm. This seems to correct the natural divergence from a single focal spot position to the detector position as positioned away from the control detector(s). Both modalities use the data from the detectors (positioned 360° around the patient) to reconstruct the axial patient images. The key difference between axial single slice CT and multi-slice is the axial image produced by single slice CT is developed from a single row of detectors, and the axial image made from a multi-slice scanner uses segments from several rows of detectors. With a multi-slice scan, as the patient moves through the gantry and the tube rotates around the patient, the detector rows utilized change as the patient and gantry move (see sketch on the next page).

Additional variables in reconstruction result as the patient slice moves from one row of detectors to the next and the scanner reconstructs the images based on weighted averages between the relevant rows. In this way, multi-slice CT is analogous to spiral or helical single slice CT, but where the reconstruction is obtained from the combined slices rather than the interpolation between the readings of a single moving slice. Now add in focal spot variables and a little scatter to define in more detail the challenges and variables included in the reconstruction of a multi-slice image.

Because in spiral mode each multi-slice image is reconstructed from an ensemble of data taken in different positions across the beam and from different detector rows, the overall image quality differences between images are minimal. In the spiral mode each slice represents data as seen from all detector rows in a sense a kind of averaging of detector row positions. However, if you use a multi-slice “step and shoot” or axial mode, where each of the slices may be created from a single detector row (or rows depending on the selected slice thickness) with a consistent collimation, the differences between the slices will be evident. Step and shoot mode in a multi-slice CT scanner is operated like a conventional axial scanner by imaging with a fixed table position and then moving the table to the next position before imaging the next section of the phantom with a fixed table position. For example, with a step and shoot 8 slice scan it is expected that the middle slice numbers 4 and 5 will have better uniformity than outer slice numbers 1 and 8 because of the scanner x-ray beam geometry. However, if 1 and 8 or 4 and 5 are not similar, this may indicate a problem with the scanner.

When assessing a scanner with a step and shoot mode, it is important to cover the full detector width with the selected test objects. If the test object is narrower than the slice, the table will need to be incremented between scanning sequences so the object can be scanned by all active rows of the detector.

I recommend scanning through the entire phantom using different multi-slice spiral protocols for performance evaluations, as well as using the step and shoot approach for the bead ramps where slice geometry and the MTF can be measured for each slice and uniformity section where the signal to noise and uniformity of each slice (detector row) can be evaluated.



This simplified illustration of a multi-slice sequence operating in spiral mode shows how the slices are reconstructed with information for different detector rows. The imaging sequence of the first selected slice (slice 1) of the patient begins when slice 1 moves over detector row A. As the tube continues to rotate and the patient continues to move through the gantry, slice 1 is picked up by the detectors in row B. At the same time slice 2, which was outside the detector view, is picked up by the detectors in row A. This sequence continues until the last selected region of the patient has passed through all the active detector rows.

## Initial phantom positioning

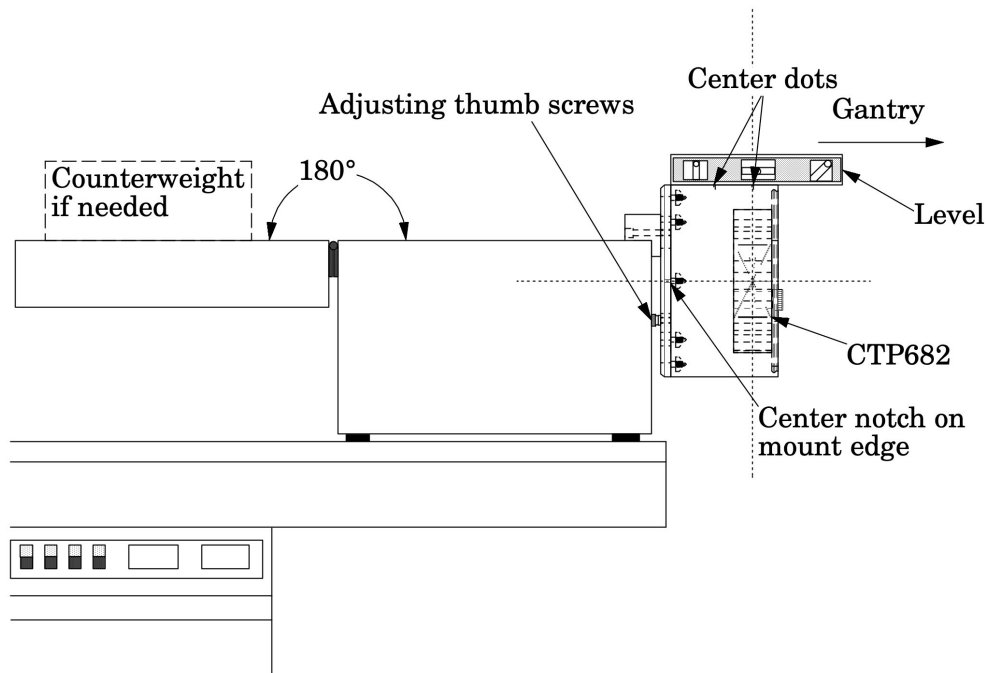
The Catphan® phantom is positioned in the CT scanner by mounting it on the case.

Place the phantom case on the gantry end of the table with the box hinges away from the gantry. It is best to place the box directly on the table and not on the table pads.

Open the box, rotating the lid back 180°. If you are using an annulus, additional weight will need to be placed in the box to counterweigh the phantom. The patient straps can be used for additional stability.

Remove the phantom from the box and hang the Catphan® from the gantry end of the box. Make sure the box is stable with the weight of the phantom and is adequately counterweighed (counterweight only required when annuli are used) to prevent tipping.

Use the level and adjusting thumb screws to level the Catphan®. Once the phantom is level, slide the phantom along the end of the box to align the center dots with the x-axis alignment light. Adjust the table height to align the height laser with the center notch on the phantom mount.

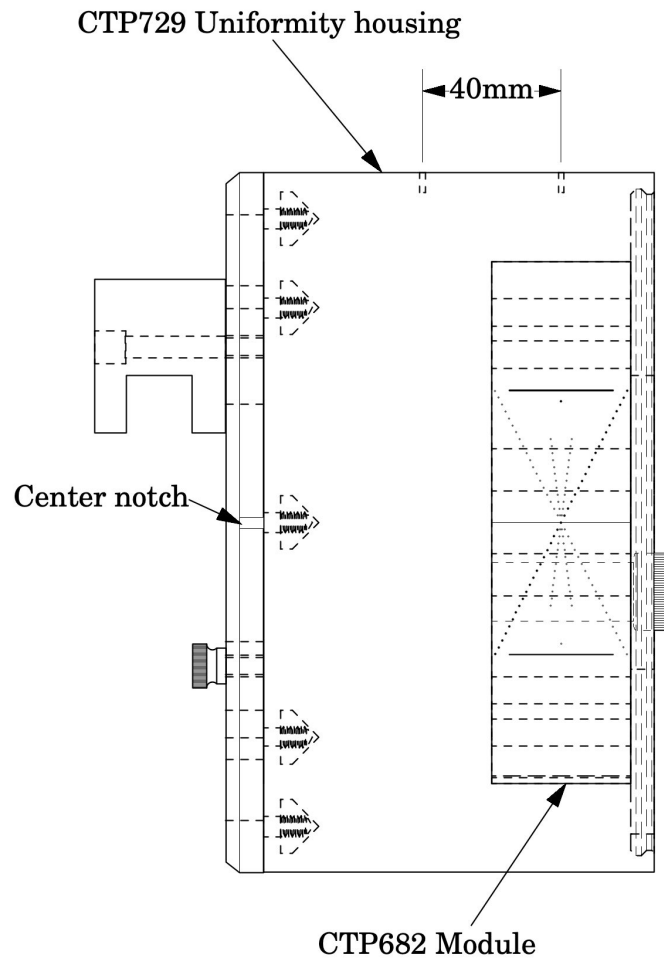


In most applications we recommend scanning through the whole phantom. Individual sections can be aligned by using a localizer scan or the center dots on the phantom.

Scan the phantom and check the CTP682 module image for proper alignment as illustrated in the **Phantom position verification** section.



### Illustration of the Catphan® 605 modules positions

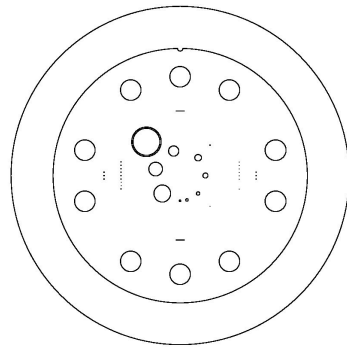


### Incremental phantom module positioning

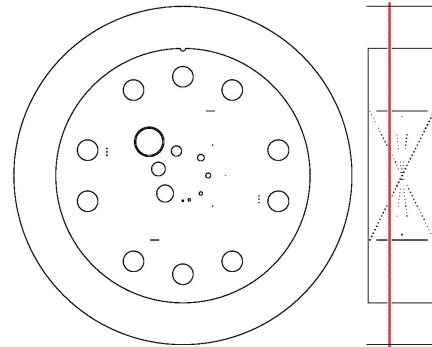
The Catphan® CTP605 phantoms are designed so all tests can be located by indexing the table 40mm from the center of CTP682 module to the center of the CTP682 module. Additional illustrations on the preceding page show the test modules and their index spacing. Phantom position verification is described on the next page.

## Phantom position verification

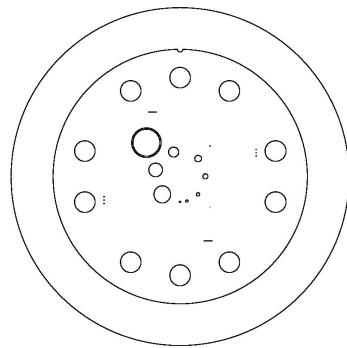
By evaluating the scan image of CTP682 the phantom's position and alignment can be verified. The section contains 2 wire ramps which rise at  $23^\circ$  angles from the base to the top of the module and 2 pairs of bead ramps. The schematic sketches below indicate how the ramp images change if the scan center is above or below the z-axis center of the test module. The use of the scanner's grid image function may assist in evaluation of phantom position.



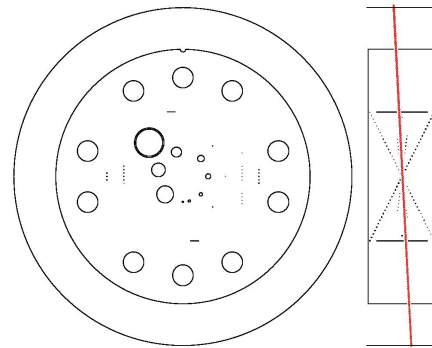
**Correct alignment**  
In this image the x y symmetry of the centered ramp images indicates proper phantom alignment



**Counter clockwise ramp skew**  
When the ramps are evenly rotated counter clockwise from center the phantom is too far into the gantry



**Clockwise ramp skew**  
When the ramps are evenly rotated clockwise from center the phantom needs to be moved towards the gantry

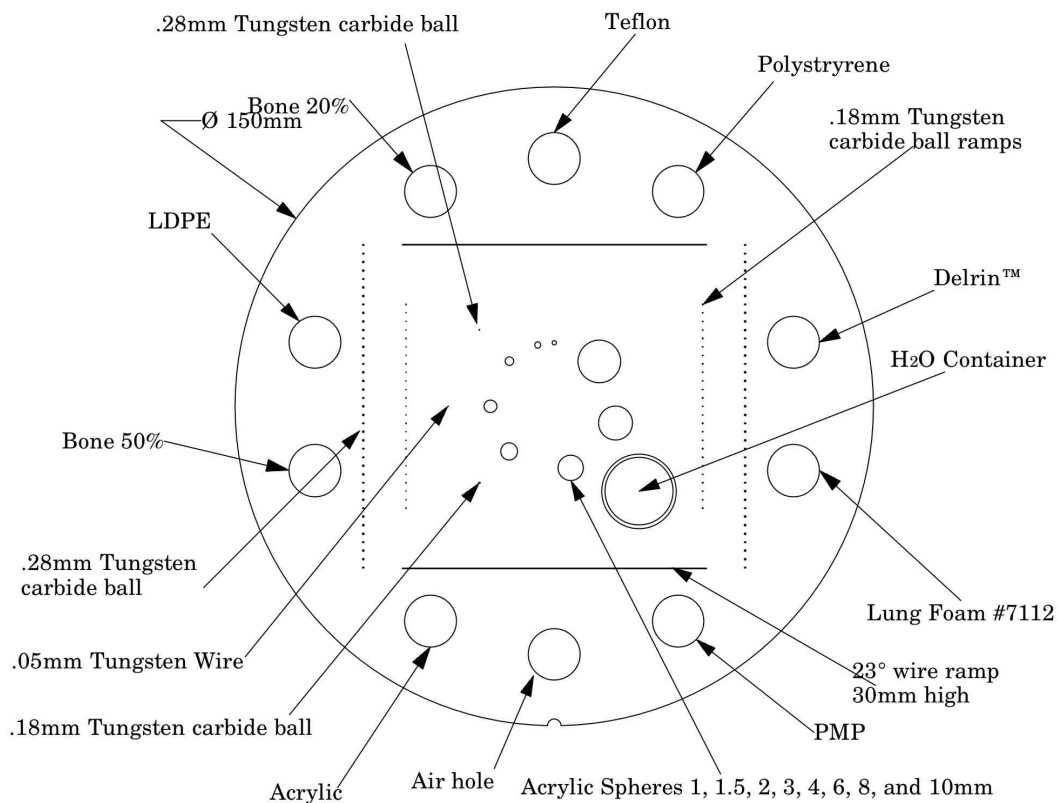


**Non symmetrical ramp images**  
Poor alignment with the z axis is indicated when the opposed ramps are not symmetrical in length and rotation

If misalignment is indicated by the scan image, the phantom should be repositioned to obtain proper alignment and then rescanned. If the images of the repositioned phantom duplicate the original misalignment indications, the scanner's alignment lights may require adjustment. See the **Patient alignment system check** section of this manual. Once correct alignment has been established, you can proceed with the tests.

### CTP682 Geometry, sensitometry module

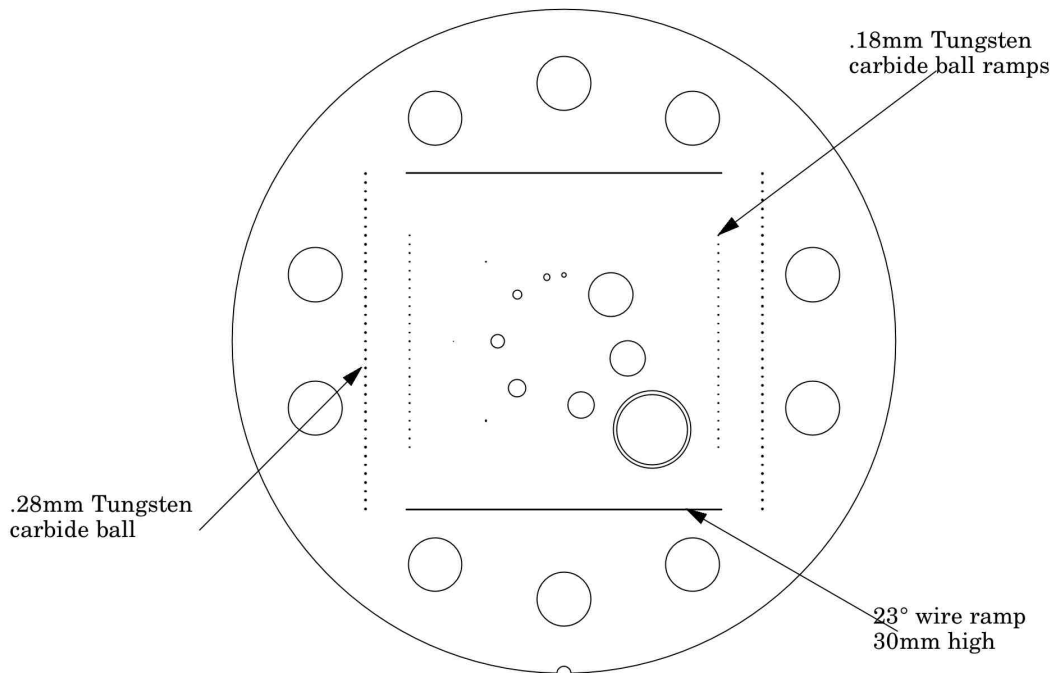
The CTP682 module is used for numerous measurements. The illustration below shows the different components. The following pages contain information on these components and their applications.



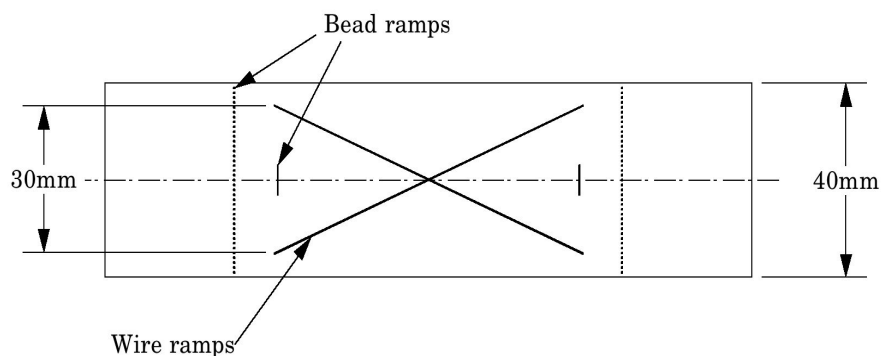
### Scan slice geometry (slice width)

The CTP682 module has a pair of  $23^\circ$  wire ramps oriented parallel to the x-axis at  $0^\circ$  rotation. These wire ramps are used to measure slice width, slice incrementation, and to check for misalignment errors as previously discussed. The use of these ramps for slice thickness and slice incrementation is discussed in the next section.

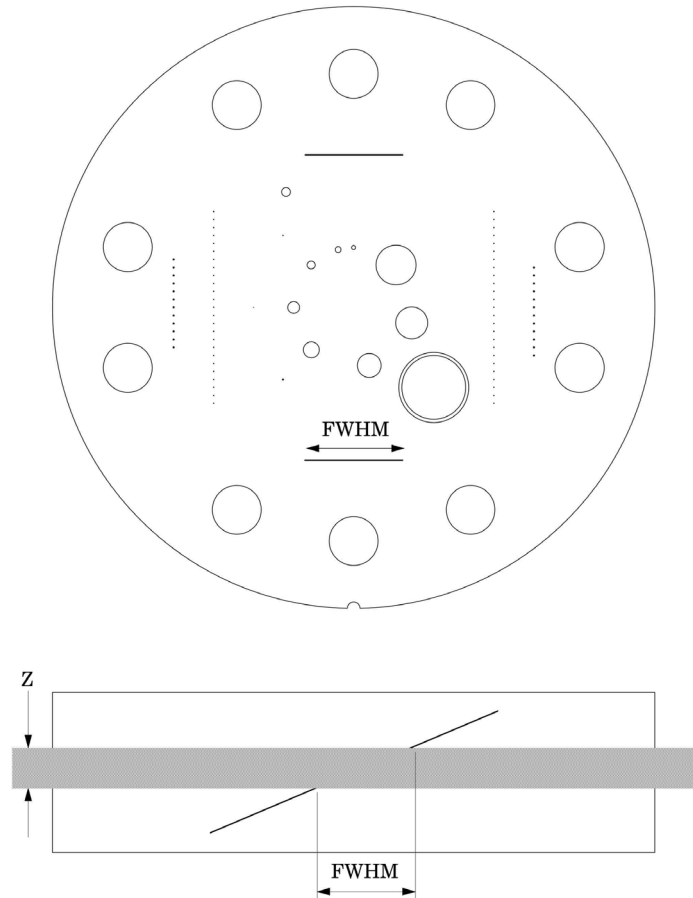
There are also two pairs of bead ramps aligned with the y-axis which, are discussed in the **Slice thickness measurement with bead ramps** section.



In the sketch below you can see the wire ramps which are positioned at  $23^\circ$  angles. You will see both ramps in the pair, which are crossing, in this side view.



### Slice width measurement with wire ramps



The 23° wire ramp angle is chosen to improve measurement precision through the trigonometric enlargement of 2.38 in the x-y image plane.

To evaluate the slice width (Zmm), measure the Full Width at Half Maximum (FWHM) length of any of the two wire ramps and multiply the length by 0.42:

$$(Zmm) = FWHM * 0.42$$

To find the FWHM of the wire from the scan image, determine the CT number values for the peak of the wire and for the background and calculate the 50% net peak.

To calculate the CT# peak of the wire, close down the CT “window” opening to 1 or the minimum setting and move the CT scanner “level” to the point where the ramp image just totally disappears. The CT number of the “level” at this position is your CT # peak.

The background CT number is measured near the ramp using the region of interest tool.

Using the above CT values, determine the half maximum:

First calculate the net peak... (CT # peak - background = net peak CT #)

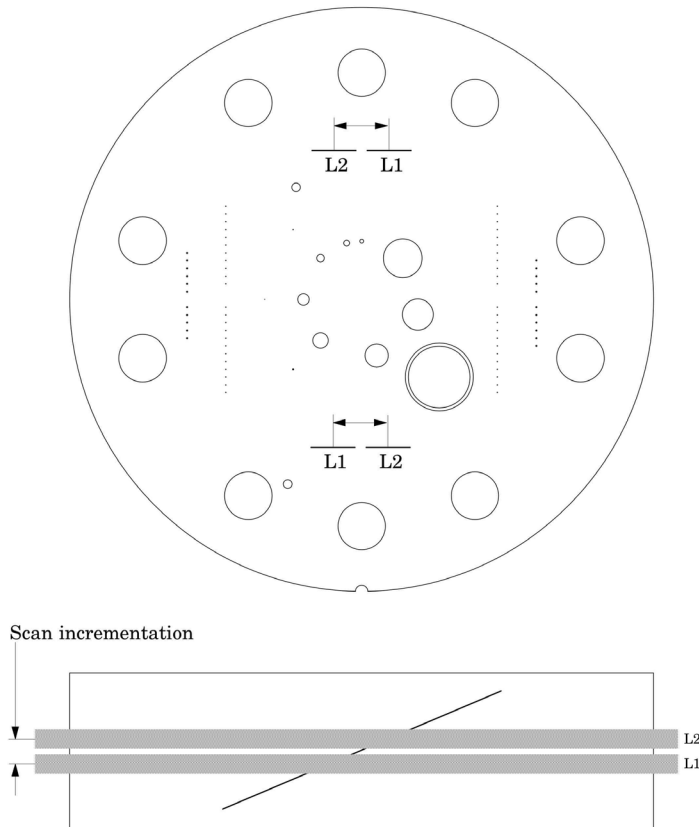
Calculate the 50% net peak... (net peak CT # ÷ 2 = 50% net peak CT #)

Calculate the half maximum CT number...

$$(50\% \text{ net peak CT \#} + \text{background CT \#} = \text{half maximum CT \#})$$

Now that the half maximum CT number is determined, measure the full width at half maximum of the ramp. Set the CT scanner level at the half maximum CT value and set your window width at 1. Measure the length of the wire image to determine the FWHM. Multiply the FWHM by 0.42 to determine the slice width.

### Scan incrementation



Schematic illustration of two sequential 5mm scans superimposed. L1 is the center point on the 23° ramp in the first scan image and L2 is the center point on the 23° ramp on the second image.

Use the wire ramps to test for proper scanner incrementation between slices, and for table movement.

Scan section 1 using a given slice width, (e.g. 5mm). Increment the table one slice width (e.g. 5mm) and make a second scan. Establish the x and y coordinates for the center of each ramp image. Calculate the distance between these points and multiply by the 23° ramp angle correction factor of 0.42.

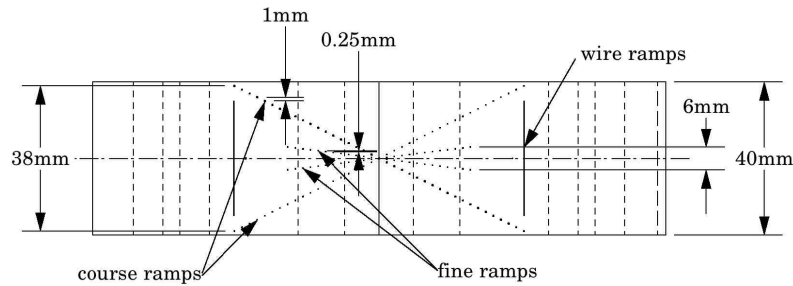
$$0.42(L1 - L2) = \text{scan incrementation}$$

This test can also be used to test table increment accuracy. Scan the section and increment the table 30mm in and out of the gantry and scan again. The ramp centers should be the same on both images.

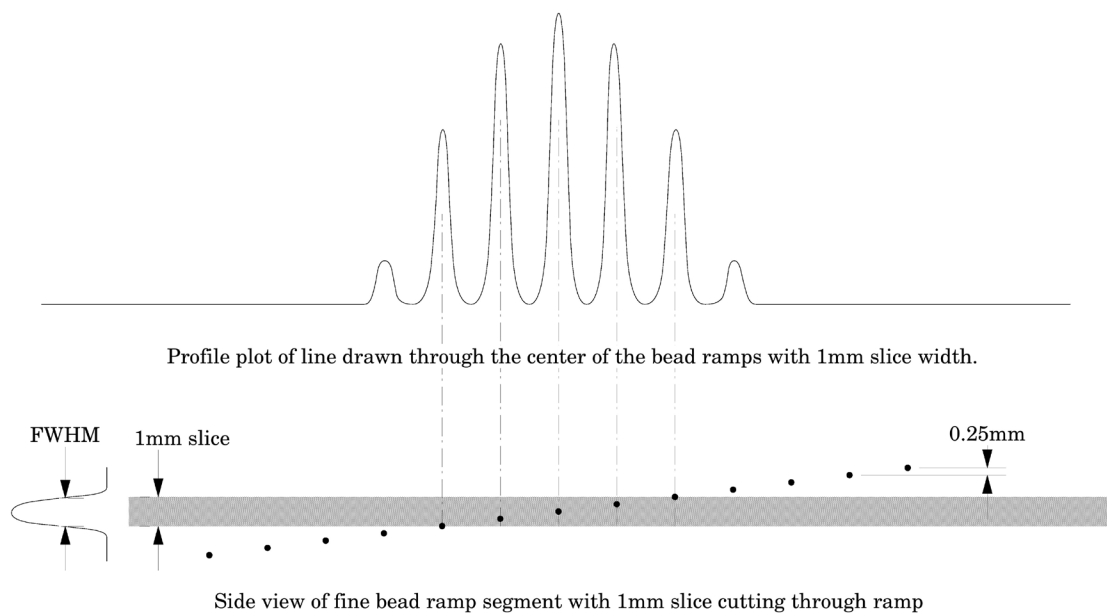
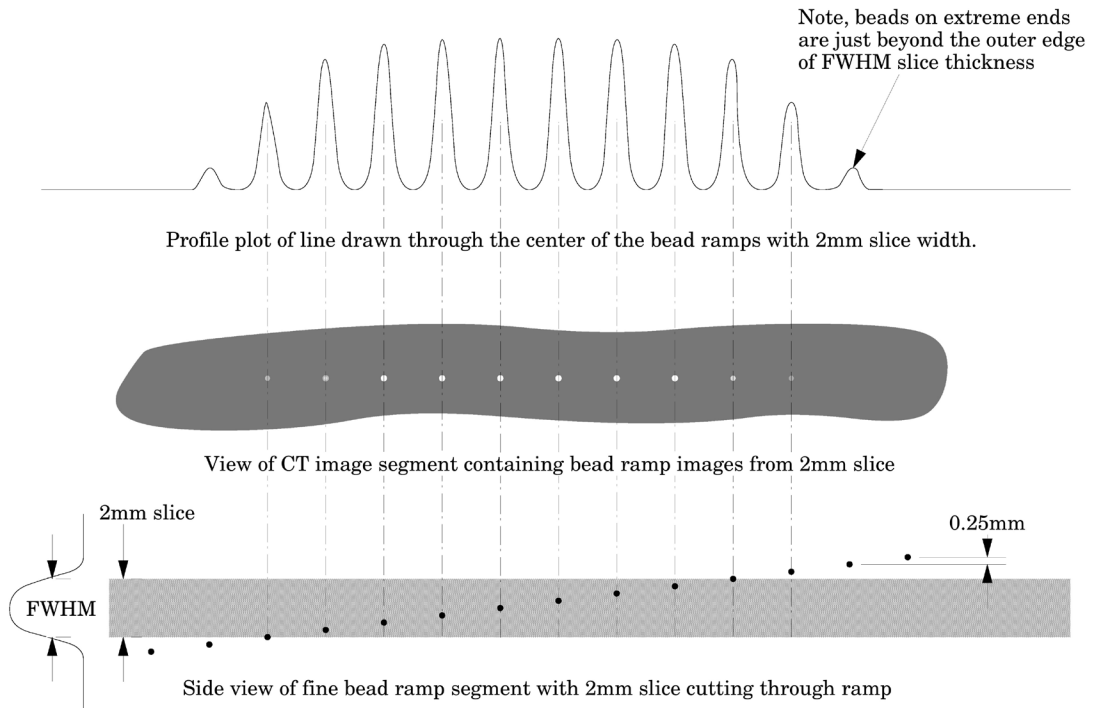
$$0.42(L1 - L2) = 0$$

### Slice width measurement with bead ramps

The CTP682 module contains 2 pairs of opposed bead ramps. The course ramp pair has 0.28mm diameter beads, spaced 1mm on center in the z direction. The fine ramp pair has 0.18mm diameter beads, spaced 0.25mm on center in the z direction. The 2 individual beads are 0.28mm and 0.18mm in diameter.



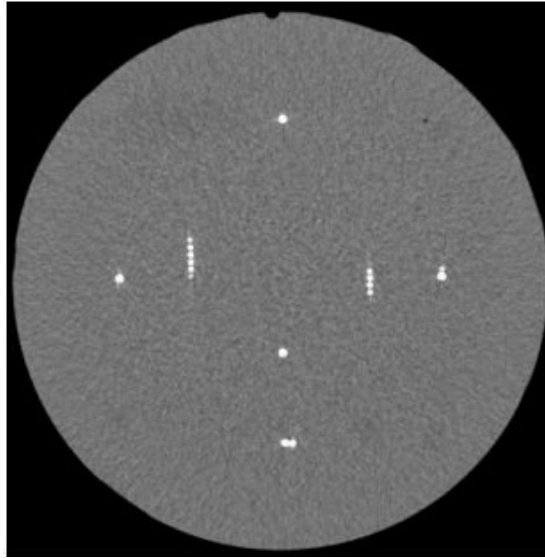
To demonstrate how the bead ramps are used, the illustration on the following page shows both a 1mm and 2mm slice going through a bead ramp. You may note that as the slice thickness increases, the peak CT value for the beads decrease. This is because as the slice thickness increases, the bead's effect on the CT number of the voxel decreases, due to volume averaging. Presuming the slice thicknesses are accurate and that the slice sensitivity profile has the same type of distribution, the peak signal over background in a 1mm slice should be approximately double that of the peak signal over the background in the 2mm slice.



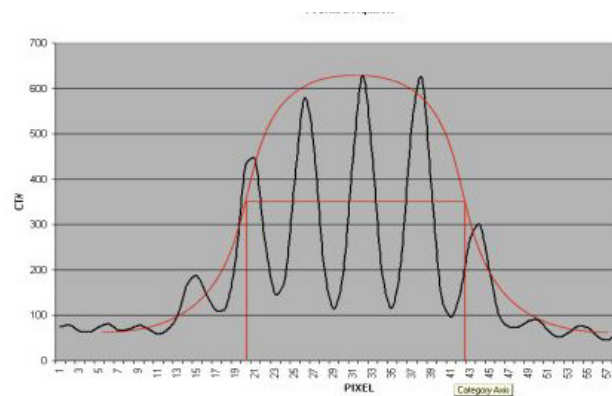


### Measuring slice thickness with a profile made from an image of the beads

Please note in this example 0.25mm spaced slice ramps are used, rather than the 1mm spaced slice ramps. The methodology for both would be basically the same, however for thinner slices the use of the fine ramps improve measurement precision. Below we use a 1mm slice scan to illustrate the use of a profile made from a line running through the bead images on the scan.



Scan of CTP591 with 1mm slice width



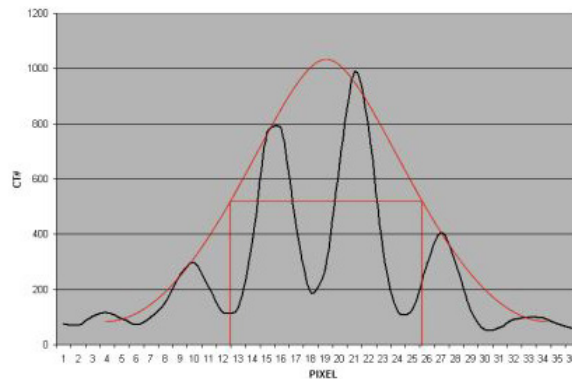
Vertical Profile of a 1mm slice through the fine .025mm bead ramps after zooming or magnification

When we use a profile line through the beads, there will be peaks at each of the bead locations and these will be separated by 0.25mm from each other in the scanner's z direction. Thus for example, for the 1.0mm slice width we measure about four bead spacings at the Full Width at Half Maximum (FWHM). Multiplying the four bead spacings times the z-axis increment 0.25mm per bead yields a 1mm slice width.

Another method for counting beads would be to measure the maximum CT number of the beads. This can be done by adjusting the window width to 1 and raising the level until the beads disappear and noting the peak level. Next, do an ROI of the area adjacent to the ramp to get a number for the background. Keeping the window width at 1, raise the level to half between background and peak (half maximum) and count the beads.

We can make this somewhat more analytic by noting the following. If we hand-draw, or use a mathematical “best fit” bell shaped curve (e.g. Gaussian) to the data points, you will notice that the peak CT number for the 1.0mm slice is about 650 H and the baseline is about 50, leaving a net value of about 600H between the peak value and the baseline. Thus,  $\frac{1}{2}$  the (net) maximum value is 300H + the baseline of about 50H so we draw a line across the 350H ordinate (Y) value and measure the length of the line that spans the two FWHM points at, in this case, 350H.

When measuring the FWHM of the curve it is important to realize that due to scaling and translation variables the scale of the FWHM length needs to be defined. This is done using the distance between the individual bead peaks in the profile whose absolute separation in the z axis is known (.25mm for fine ramps and 1mm for course ramps). For example for the fine ramps divide the FWHM by the distance between bead peaks and multiply by .25mm.



Vertical Profile of a 0.5mm slice through the fine .025mm bead ramps after zooming or magnification

Please note, the typical tolerance allowed is somewhere between 0.5mm and 10% depending on the vendor, and the slice thickness being measured.

### **Additional methods for estimating and measuring slice thicknesses with the bead ramps**

A slice sensitivity profile (SSP) of the bead(s) can be used to measure slice thickness (see the **Bead point source** section for additional information).

Sagittal and coronal slices through the beads can also be used to measure the axial slice width. In this case measure the z-axis length at the full width at half maximum of a bead image to establish the slice thickness. However, this technique is limited in precision z-axis of the voxels.

The volume averaging effect on the net peak CT number of the bead can be used to approximate additional slice thickness measurements after measuring one slice's thickness by using the following equation:

- w = slice width of additional slice thickness.
- npvm = net peak value of the bead in the measured slice width
- msw = slice width of the measured slice
- npva = net peak value of the bead in the additional slice width

$$w = (npvm / npva) * msw$$

Note: Net peak value = (CT# of the bead) - (CT# of the background)

### Patient alignment system check

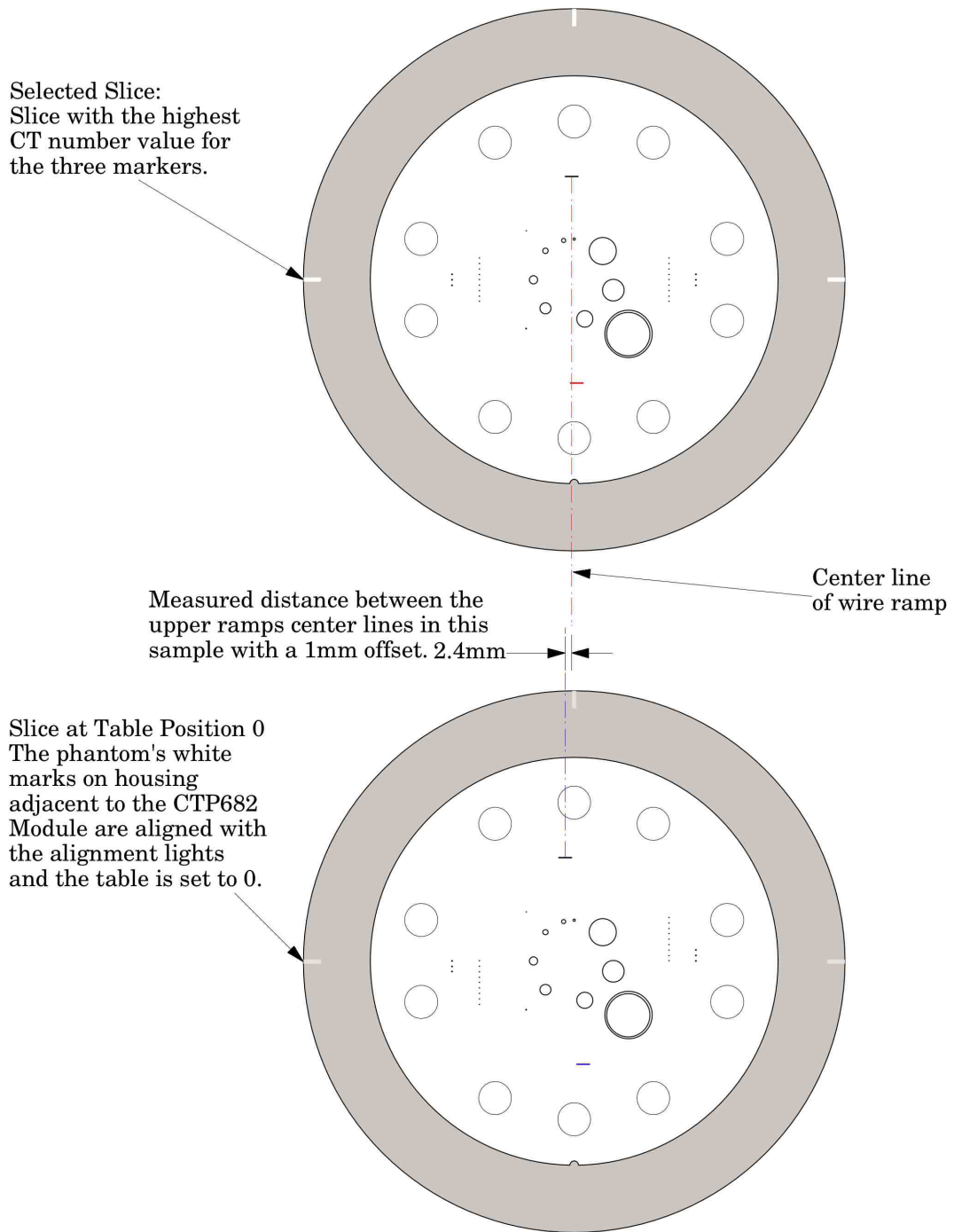
The patient alignment lights can be checked for accuracy by using the white alignment markers on the phantom housing. Align the phantom as discussed in **Initial phantom positioning** and set the table position at 0. Please note that due to housing casting variations the alignment markers may be off by a couple millimeters from the center of the CTP682 module. For a quick check scan through the phantom at the 0 table position and check to see if you are in the center of the module.

For a more precise measurement, scan through the module using the thinnest available slice width. Scroll through the slices and select the slice with the highest CT value for the 3 alignment markers. Check the table position of the “selected slice”, if it is 0 your alignment lights are accurate, if the table position of the “selected slice” is different from the slice with a table position 0 then the alignment will be off by the distance from the 0 table position slice to the “selected slice”. The distance between the center of the two slices can also be measured by measuring the distance between lines running through the center of the ramp images in the two slices and multiplying this distance by  $.42, \tan(23^\circ)$ , the ramp scaling factor. See illustration on the next page.

It is important to note that with some multi-slice, when an even number of slices is used, scanners the slice is not centered at zero. Instead the slice starts at zero. In this case the slice center will be  $1/2$  the slice width away from the zero position.

To evaluate x and y accuracy, measure from the center of the phantom to the center of the scan field by use of the grid function or knowledge of the central pixel location.

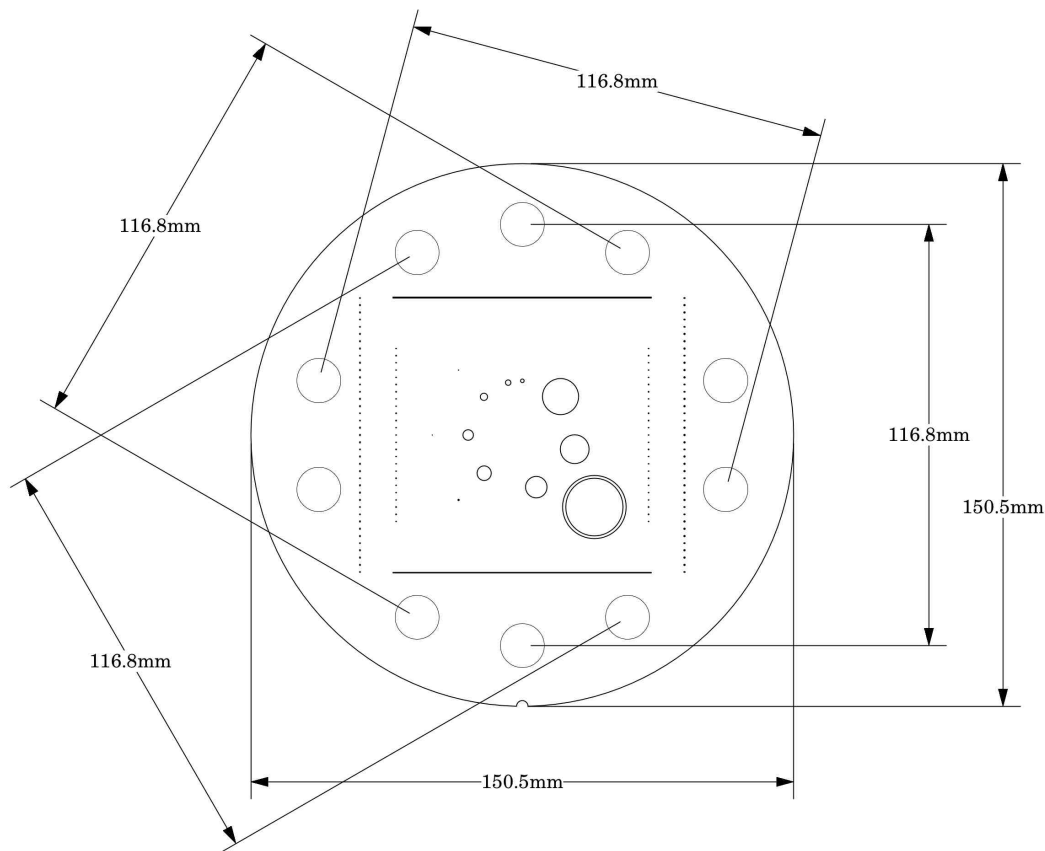
The accuracy of the localizer, pilot or scout view can be checked. To check this function perform a localization scan of the phantom. Align an axial scan at the crossing point of the wire ramps. Set this location of the table to 0. Scan through the CTP682 module using the thinnest available slices. Select the slice where the ramps are closest to the center. Compare this slice with the slice at the table position 0 as described above to measure the offset.



$$(\text{measured distance between center lines}) \times 0.42 (\tan(23^\circ) \text{ ramp scaling factor}) = \text{z axis alignment light offset}$$

### Circular symmetry of display system

The circular phantom sections are used to test for circular symmetry of the CT image, including calibration of the CT display system. If an elliptical image is produced, the x-y balance of the image display system should be adjusted.

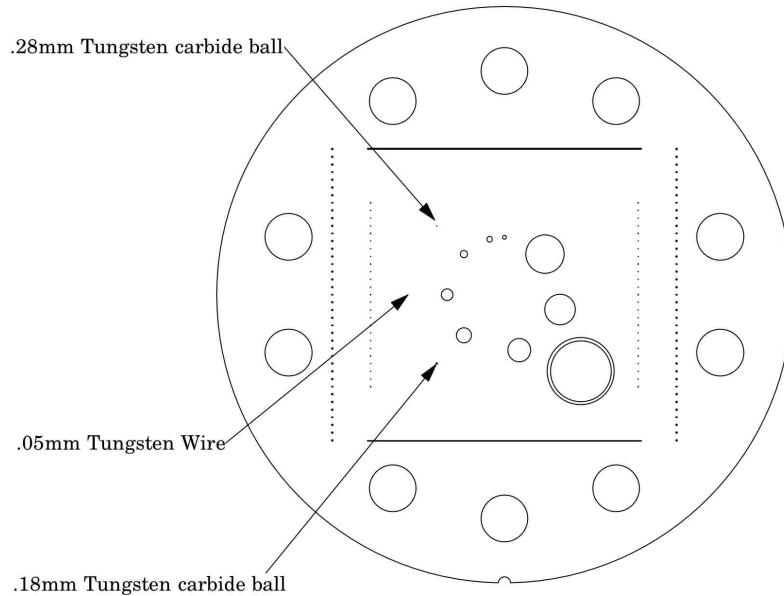


Measuring spatial linearity

### Spatial linearity and pixel size verification

The diameter of the module in the x and y-axes can be measured to verify the scanners spatial linearity. This section has ten holes (with sensitometry targets). These 12.2mm diameter holes provide 5 diametrically opposed pairs measuring, center to center, 116.8mm apart. By measuring from center to center between the holes, or the diameter of the module, the spatial linearity of the CT scanner can be verified. Another use is to count the number of pixels between the hole centers. By knowing the distance and number of pixels, the pixel size can be verified.

### Bead or wire point source for determination of point spread function and MTF

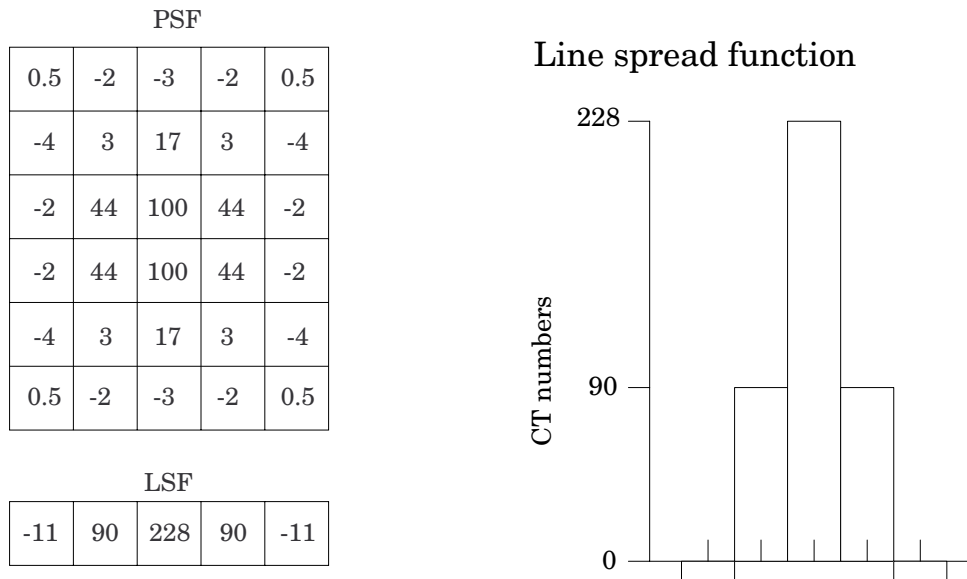


Use the bead or wire impulse source to estimate the point source response function of the CT system. Print out a digitized image of the area surrounding the impulse source. Use the numerical data to determine the two-dimensional array of the CT values arising from the impulse source.

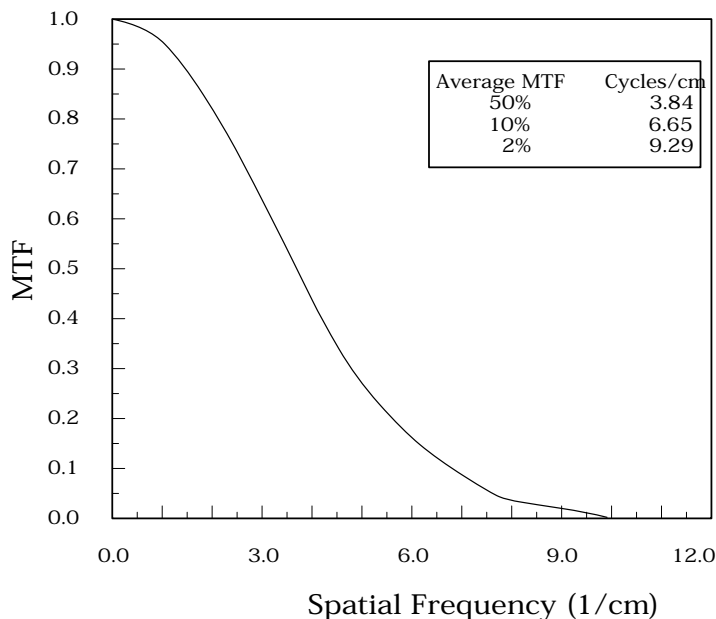
The FWHM of the point spread function is determined from the best-fit curve of the point spread function numerical data.

The average of several different arrays of impulse response functions is calculated to obtain the average point spread function of the system. These numerical values are used in conjunction with the Fourier Transform Program to provide an estimate of the two-dimensional spatial frequency response characteristics of the CT system (MTF). An illustration is on the next page.

The tungsten carbide bead has a diameter of 0.011" or 0.28mm. Because the bead is subpixel sized it is not usually necessary to compensate for it. However, some MTF programs are designed to compensate for its size.



The above illustration shows how by summing the columns (y-axis) of pixel numbers in the point spread function (PSF) the line spread function (LSF) for the x-axis is obtained. Likewise the (LSF) for the y-axis can be obtained by summing the rows (x-axis) data.



The MTF curve results from the Fourier Transform of the LSF data. Generally it is easiest to use automated software for this operation. Some CT scanners are supplied with software which can calculate the MTF from the Catphan® bead images. Independent software is listed in the **Current automated programs available** section of the manual.

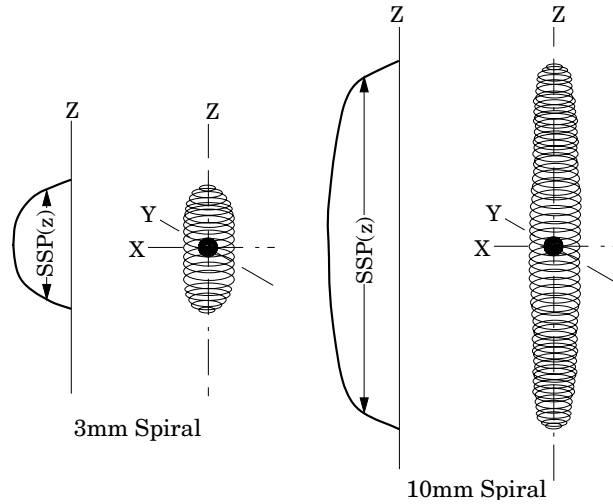
#### Use of automated scanner MTF programs

Many manufacturers include automated MTF software in the standard scanner software packages. Because the bead is cast into an urethane background which has a different density than water, the software must accept an input for the background CT number. The automated Image Owl and Oncology Owl services automatically corrects for the background value in PSF and MTF calculations. The point size of .28mm for the large bead, .18mm for the small bead or .05mm for the wire must also be selected. While a sphere does produce a different density profile than a cross section of a wire or cylinder,

both objects are so small that the actual difference is not usually significant in current CT scanners.

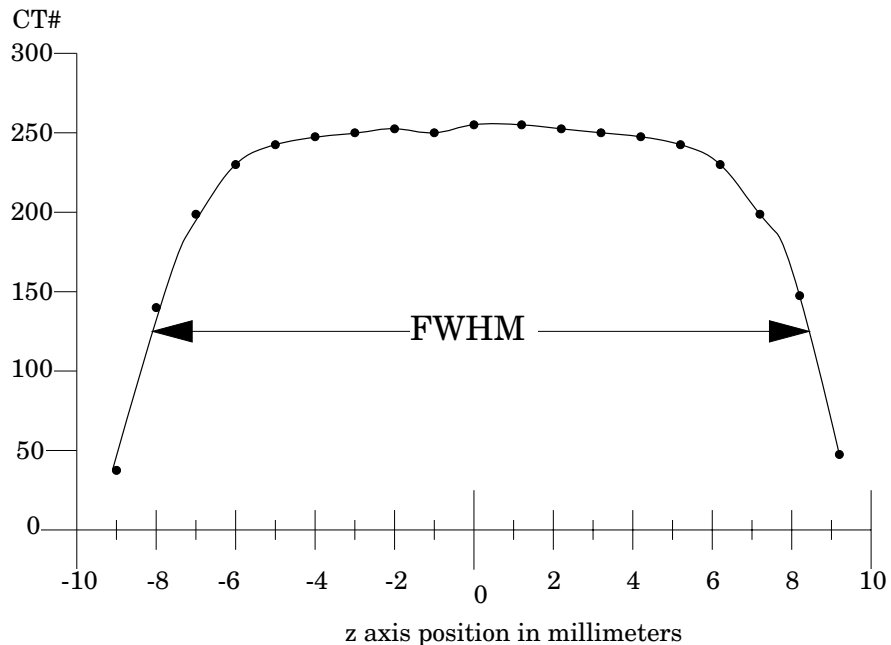
### Bead point source for slice sensitivity profile

The bead in this module can be used to calculate the slice sensitivity profile (SSP).



The above image illustrates how the bead will produce an ovoid object in a 3 dimensional reconstruction. The length of the object at the Full Width at Half Maximum signal indicates the SSP. This measurement can be easily obtained on some systems, by making a sagittal or coronal reconstruction through the bead. The bead image in these reconstructions will appear as a small line. By setting the FWHM (use the same technique described in the **Scan slice geometry** section) measuring the z-axis length of the bead image to obtain the SSP.

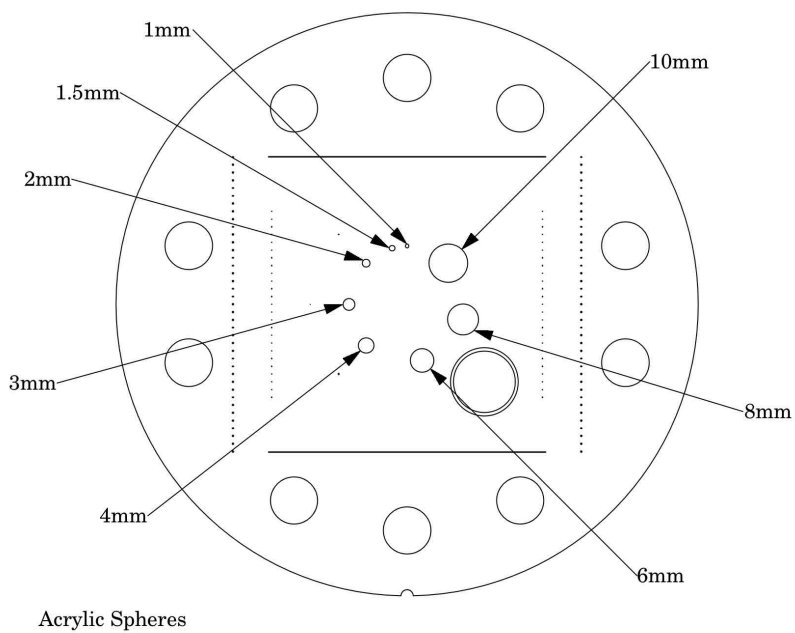
If the scanner does not have the ability to measure z-axis lengths in the sagittal or coronal planes, a SSP can be made by incrementing or spiraling the slice through the bead and reconstructing images in positive and negative table directions from the bead (using the smallest available increments) and plotting the peak CT number of the bead image in each slice. The FWHM measurement can then be made from the plotted CT values of the bead as a function of z-axis table position.





### Spherical acrylic contrast targets

The CTP682 module has 8 acrylic spheres located in a 30mm diameter circular pattern. These spheres are used to evaluate the scanner's ability to image volume averaged spheres. The sphere diameters are 1, 1.5, 2, 3, 4, 6, 8, and 10mm.



## CT or Hounsfield Numbers by David Goodenough, Ph.D.

Users of CT systems are often surprised when the CT number of a given tissue or substance is different from what they expect from previous experience. These differences do not usually indicate problems of a given CT scanner, but more likely arise from the fact that CT numbers are not universal. They vary depending on the particular energy, filtration, object size and calibration schemes used in a given scanner. One of the problems is that we are all taught that the CT number is given by the equation:

$$CT\# = k(\mu - \mu_w)/\mu_w,$$

where  $k$  is the weighting constant (1000 is for Hounsfield Scale),  $\mu$  is the linear attenuation coefficient of the substance of interest, and  $\mu_w$  is the linear attenuation coefficient of water. Close review of the physics reveals that although the above equation is true to first order, it is not totally correct for a practical CT scanner. In practice,  $\mu$  and  $\mu_w$  are functions of energy, typical x-ray spectra are not monoenergetic but polychromatic, and a given spectrum emitted by the tube is “hardened” as it is transmitted (passes) through filter(s) and the object, finally reaching the detector. More accurately,  $\mu = \mu(E)$ , a function of energy. Therefore:

$$CT\#(E) = k(\mu(E) - \mu_w(E))/\mu_w(E)$$

Because the spectrum is polychromatic we can at best assign some “effective energy”  $\hat{E}$  to the beam (typically some 50% to 60% of the peak kV or kVp). Additionally, the CT detector will have some energy dependence, and the scatter contribution (dependent on beam width and scanned object size, shape, and composition) may further complicate matters. Although the CT scanner has a built in calibration scheme that tries to correct for beam hardening and other factors, this is based on models and calibration phantoms that are usually round and uniformly filled with water, and will not generally match the body “habitus” (size, shape, etc.).

The situation is really so complicated that it is remarkable that tissue CT numbers are in some first order ways “portable”!

In light of the above we can examine a parameter of CT performance, the “linearity scale”, as required by the FDA for CT manufacturer’s performance specifications.

The linearity scale is the best fit relationship between the CT numbers and the corresponding  $\mu$  values at the effective energy  $\hat{E}$  of the x-ray beam.

The effective energy  $\hat{E}$  is determined by minimizing the residuals in a best-fit straight line relationship between CT numbers and the corresponding  $\mu$  values.

In review, we will encounter considerable inter and intra scanner CT number variability. CT numbers can easily vary by 10 or more based on kVp, slice thickness, and object size, shape, and composition. There is some possibility of the use of iterative techniques and/or dual energy approaches that might lessen these effects, but certainly CT numbers are not strictly portable and vary according to the factors listed above.

More complete scientific references are contained in the bibliography. In particular, references 2, 13, 14, and 20 are recommended for those with greater interest in the topic.

### Sensitometry (CT number linearity)

The CTP682 module has sensitometry targets made from Teflon®, Bone 50%, Delrin®, Bone 20%, acrylic, Polystyrene and low density polyethylene (LDPE), polymethylpentene (PMP), Lung foam #7112 and air. The module is also equipped with a small removable vial which can be filled with water or other material and inserted into the CTP682 module.

These targets range from approximately +1000 HU to -1000 HU. A table with the linear attenuation coefficient  $\mu$  [units  $\text{cm}^{-1}$ ] can be downloaded from our web site.

The monitoring of sensitometry target values over time can provide valuable information, indicating changes in scanner performance. Note, values can change depending on local temperature and pressure.

#### Nominal material formulation and specific gravity

Material	Formula	$Z_{\text{eff}}^1$	Specific Gravity <sup>2</sup>	HU range <sup>3</sup>
Air	.78N, .21O, .01Ar	8.00	0.00	-1046 : -986
Lung #7112	[C <sub>38</sub> H <sub>38</sub> N <sub>8</sub> O <sub>15</sub> ]	6.64	0.19	-925 : -810
PMP	[C <sub>6</sub> H <sub>12</sub> (CH <sub>2</sub> )]	5.44	0.83	-220 : -172
LDPE	[C <sub>2</sub> H <sub>4</sub> ]	5.44	0.92	-121 : -87
Water	[H <sub>2</sub> O]	7.42	1.00	-7 : 7
Polystyrene	[C <sub>8</sub> H <sub>8</sub> ]	5.70	1.03	-65 : -29
Acrylic	[C <sub>5</sub> H <sub>8</sub> O <sub>2</sub> ]	6.47	1.18	92 : 137
Bone 20%	.51C, .06Ca, .06H, .06N, .30O, .03P	9.09	1.14	211 : 263
Delrin®	Proprietary	6.95	1.42	344 : 387
Bone 50%	.35C, .14Ca, .04H, .06N, .34O, .06P	11.46	1.40	667 : 783
Teflon®	[CF <sub>2</sub> ]	8.43	2.16	941 : 1060

#### Electron density and relative electron density

Material	Electron Density ( $10^{23}$ e/g)	Electron Density ( $10^{23}$ e/cm <sup>3</sup> )	Relative Electron Density <sup>4</sup>
Air	3.002	0.004	0.001
Lung #7112	3.144	0.588	0.176
PMP <sup>5</sup>	3.435	2.851	0.853
LDPE <sup>6</sup>	3.435	3.160	0.945
Water	3.343	3.343	1.000
Polystyrene	3.238	3.335	0.998
Acrylic	3.248	3.833	1.147
Bone 20%	3.178	3.623	1.084
Delrin®	3.209	4.557	1.363
Bone 50%	3.134	4.387	1.312
Teflon®	2.890	6.243	1.868

<sup>1</sup>  $Z_{\text{eff}}$ , the effective atomic number, is calculated using a power law approximation.

<sup>2</sup> For standard material sensitometry inserts The Phantom Laboratory purchases a multiple year supply of material from a single batch. Samples of the purchased material are then measured to determine the actual specific gravity. The specific gravity of air is taken to be .0013 at standard temperature and pressure. For custom cast materials the specific gravity of each cast batch is noted and supplied with the phantom. The lung #7112 is a foam, and while it is purchased in large batches it varies throughout the batch. For this reason the lung numbers may have a greater variation.

<sup>3</sup> These are maximum and minimum measured values from a sample of 94 scans using different scanners and protocols. HU can vary dramatically between scanners and imaging protocols and numbers outside of this range are not unusual.

<sup>4</sup> Relative Electron Density is the electron density of the material in  $e/cm^3$  divided by the electron density of water ( $H_2O$ ) in  $e/cm^3$ .

<sup>5</sup> Polymethylpentene

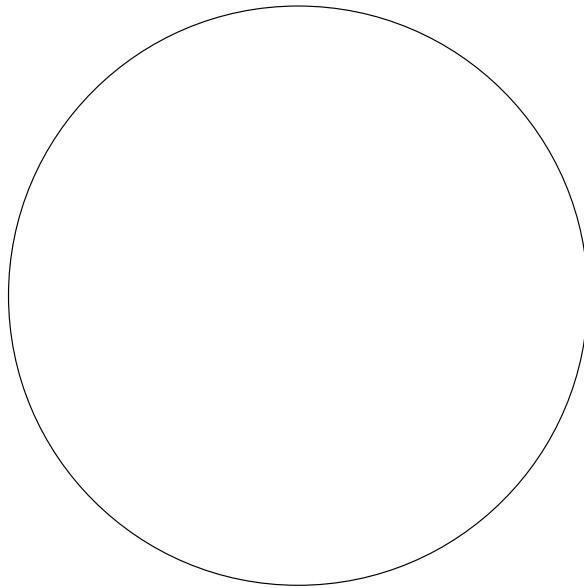
<sup>6</sup> Low Density Polyethylene

An excel file with the linear attenuation coefficient  $\mu$  [units  $cm^{-1}$ ] for the sensitometry materials can be downloaded from our web site.

### **Filling the water vial**

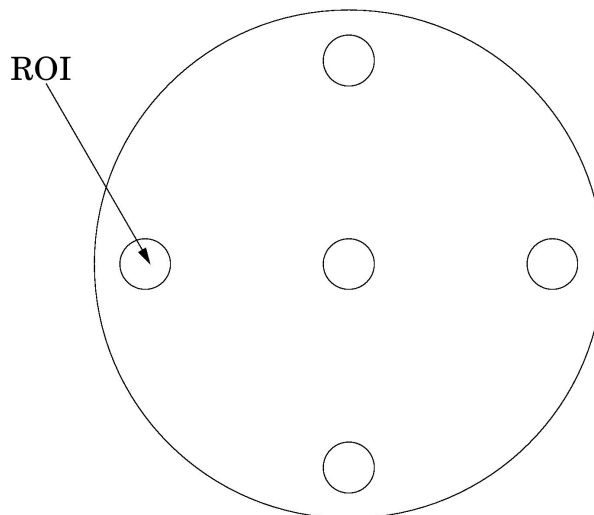
To fill the water vial, pull the vial out of the phantom and remove the lid. The use of distilled water eliminates possible variables due to tap water purity. Submerge the container and lid under water and position so all air escapes then tighten the lid onto the vial preventing air from entering the vial. Dry off the vial and insert it back into the CTP682 module. Check that no air bubbles remain in the vial and allow the vial to return to normal room temperature.

### CTP729 Image uniformity module



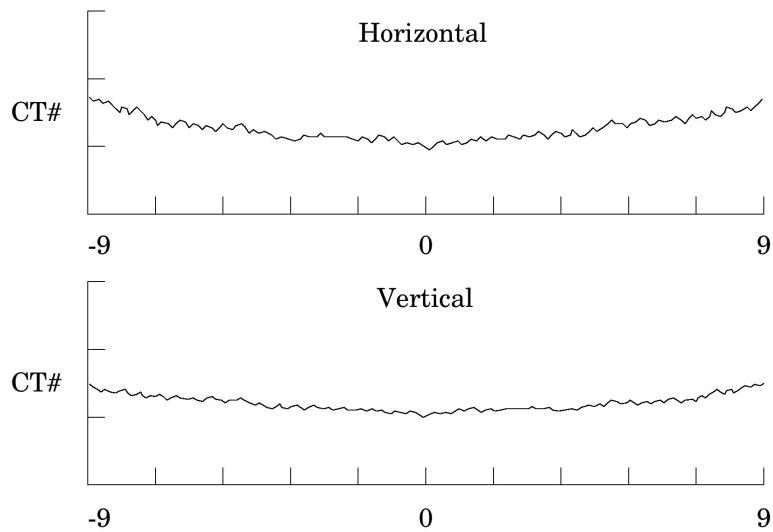
The image uniformity module is cast from a uniform material. The material's CT number is designed to be within 2% (20H) of water's density at standard temperature and standard scanning protocols. The typically recorded CT numbers range from -5H to 18H. This module is used for measurements of spatial uniformity, mean CT number and noise value.

The precision of a CT system is evaluated by the measurement of the mean value and the corresponding standard deviations in CT numbers within a region of interest (ROI). These measurements are taken from different locations within the image uniformity module. The deviation from the central mean ROI and or the mean value over the module as a whole (excluding the region near the boundary of the object) is measured.



The mean CT number and standard deviation of a large number of points, (say 1000 for example) in a given ROI of the scan, is determined for central and peripheral locations within the scan image for each type of scanning protocol.

Inspect the data for changes from previous scans and for correlation between neighboring slices.



Measure spatial uniformity by scanning the uniformity section. Observe the trends above and below the central mean value of a CT number profile for one or several rows or columns of pixels as shown above.

Select a profile which runs from one side of the uniformity module to the opposite side. Due to scanner boundary effects, typical profiles start one ROI, or about 2cm, from the edge of the test module.

Integral uniformity may be measured by determining the minimum and maximum CT values along the profile and by using the following equation :

$$\text{Integral Non-Uniformity} = \frac{\text{CT}_{\text{max}} - \text{CT}_{\text{min}}}{\text{CT}_{\text{max}} + \text{CT}_{\text{min}}}$$

$$\text{Integral Uniformity} = 1 - (\text{Integral Non-Uniformity})$$

The phenomenon of “cupping” or “capping” of the CT number may indicate the need for recalibration.

### **Automated computer analysis program**

To assist our customers, The Phantom Laboratory has worked with Image Owl, Inc. to develop a web-based automated service. The Image Owl Catphan® QA service offers detailed CT performance testing and reports with the versatility of Internet access. This service can be used with Catphan® 500, 503, 504, 600, 605, and 700 models.

The Phantom Laboratory provides for free a single slice upload version of the service. Image Owl offers additional advanced tools and services, including longitudinal history, with a subscription to the service.

Test reports include:

- Spatial resolution (modulation transfer function)
- Noise and image uniformity
- Slice width and pixel size
- Sensitometry (CT# linearity, input - output relationship)
- Contrast detectability (C-D model)

Please contact Image Owl for information on the services available.

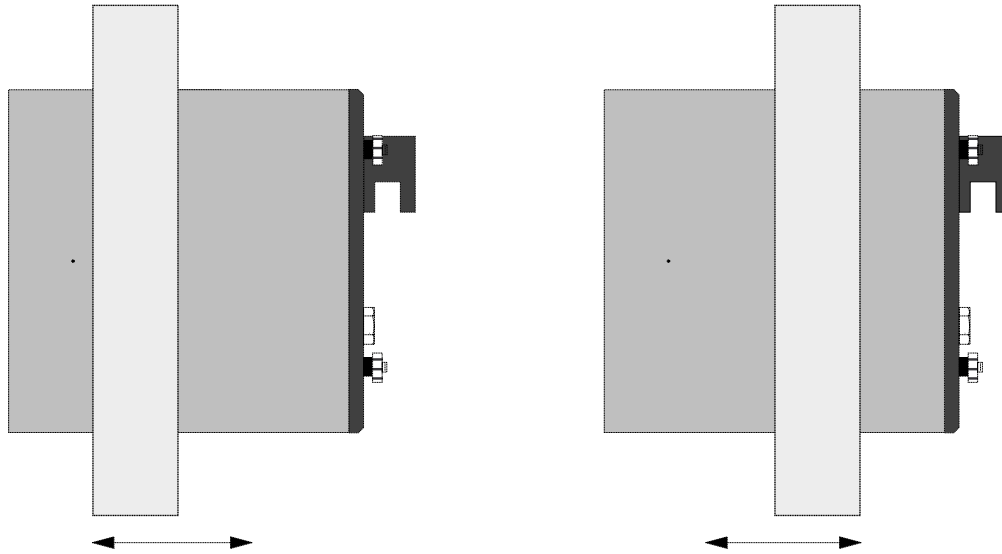
[www.imageowl.com](http://www.imageowl.com)

[info@imageowl.com](mailto:info@imageowl.com)

### Optional phantom annuli

#### Warning

Before mounting a Catphan® phantom with an annulus onto the Catphan® case, the case must be secured to the table by use of the patient restraint straps or additional counterweight. If the case is not secured to the table when the phantom is mounted, the case, phantom and annulus could fall off the edge of the table. Because the annulus adds extra weight to the phantom check to see if the phantom is still level and adjust the leveling screw as required.



The following optional annuli are designed to be used with the standard 20cm Catphan® housing.

- CTP299 21.5cm diameter, Teflon annulus simulates the high absorption of bone.
- CTP539 30cm diameter annulus, cast from the image uniformity material.
- CTP540 35cm diameter annulus, cast from the image uniformity material.
- CTP650 38cm diameter annulus, cast from the image uniformity material.
- CTP579 25-35cm OD oval annulus, cast from the image uniformity material.
- CTP651 30-38cm OD oval annulus, cast from the image uniformity material.
- CTP599 45-55cm OD oval annulus, cast from the image uniformity material.

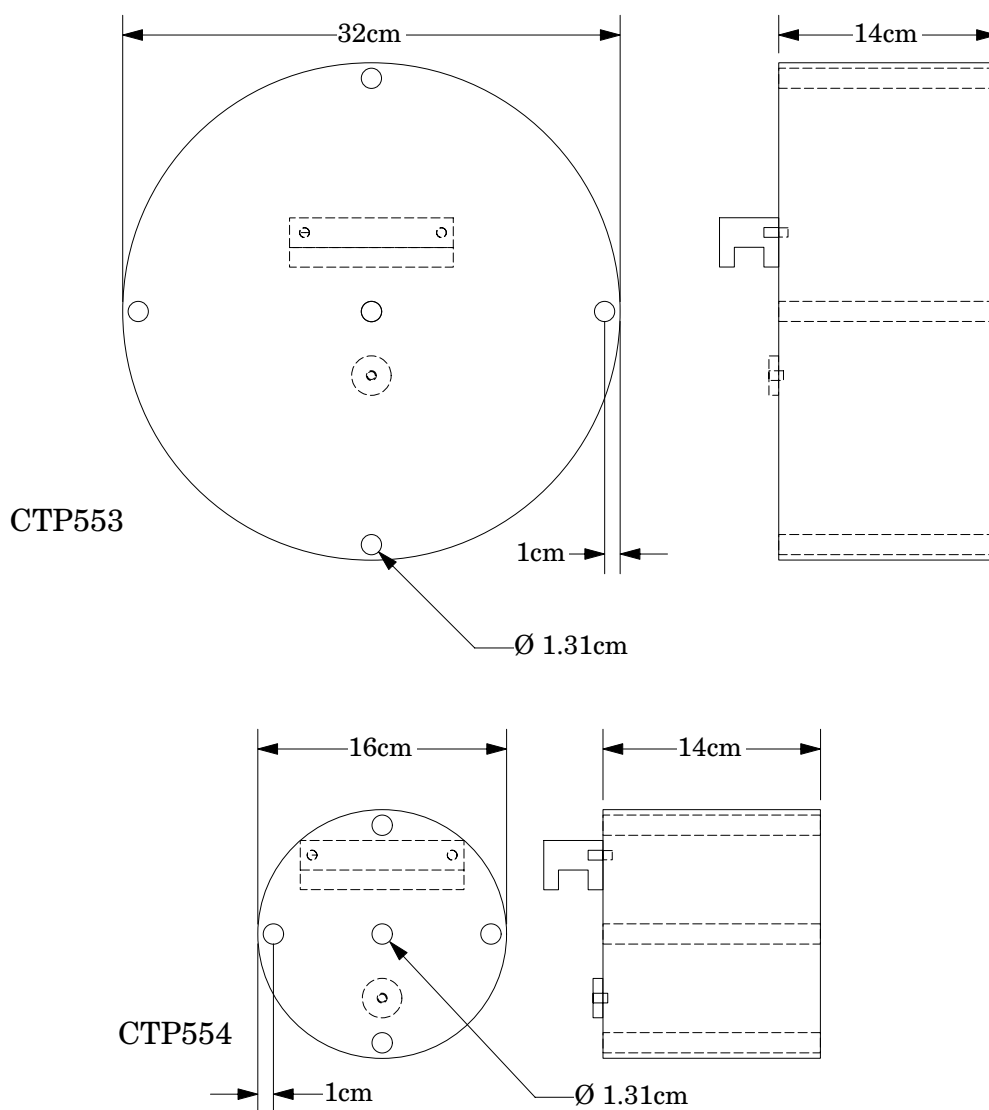
The annuli are designed to slide over the 20cm Catphan® housing as illustrated below. Because the housing material and the uniformity annuli lack lubricity, the annuli may not slide easily. However, by adding some non-metallic water or silicone based lubricant the resistance can be reduced.



## Dose Phantoms

The CTP553 and CTP554 dose phantoms are designed to the Food and Drug Administration's Center for Devices and Radiological Health specification, listed in 1020.33.

The dose phantoms may be mounted on the Catphan® case following the same procedures and precautions used in initial phantom positioning. The holes will accept a 1/2" or 13mm diameter dose probe.



### Warning

Make sure the Catphan® case is secure and additional counterweight may be required before mounting 32cm dose module onto case.

**Sample quality assurance program**

The following shows a sample QA program. Review the local governing requirements, and the needs of your physicians and physicists when developing a QA program for your institution. This program should only be utilized as an example.

All tests should be conducted at initial acceptance and after major repair such as tube replacement. Perform the weekly tests after each preventative maintenance.

## Suggested frequency of tests:

	Daily	Weekly	Monthly*
Positional verification	•	•	•
Circular symmetry			•
Scan slice geometry		•	•
Impulse response function			•
Resolution		•	•
Low contrast		•	•
Contrast sensitivity		•	•
Uniformity and noise characteristics	•	•	•

\*Or following preventative maintenance

## Bibliography

1. AAPM Report No. 39  
Specification and Acceptance Testing of Computed Tomography Scanners  
Report of Task Group 2 Diagnostic X-Ray Imaging Committee. Published for the  
American Association of Physicists in Medicine by the American Institute of Physics.  
May 1993
2. M. J. Berger, J. H. Hubbell, S. M. Seltzer, J. Chang, J. S. Coursey, R. Sukumar, and D.  
S. Zucker, Feb. 2009, XCOM: Photon Cross Sections Database, NIST Standard Reference  
Database 8 (XGAM), <http://www.nist.gov/physlab/data/xcom/index.cfm> (July 7, 2010).
3. Brooks and DiChiro  
Principles of Computer Assisted Tomography (CAT) in Radiographic and  
Radioisotopic Imaging  
Phys Med Biol 1976;21:689-732
4. Cohen and DiBanca  
The Use of Contrast-Detail-Dose Evaluation of Image Quality in a Computed  
Tomographic Scanner  
Comput. Assist. Tomogr. 3, 189-195 1979
5. Goodenough  
Volume Tomographic Imaging (Chapter 8)  
In: Bentel, Kundel, Van Metter (eds). Handbook of Medical Imaging, Volume 1: Progress  
in Medical Physics and Psychophysics.  
Bellingham, Washington, 2000: 511-554
6. Goodenough  
Assessment of Image Quality of Diagnostic Imaging Systems  
In: Gray GA (ed). Medical images: formation, perception and measurements. Proceedings  
of the 7th L.H.Gray Conference, New York: John Wiley & Sons, 1976:263-77
7. Goodenough  
Automated Quality Assurance for CT Scanners  
(Chapter): Radiology ICR 749, Editors Silver, Abecasis and Veiga-Pires. Excerpta Medica  
Press, Amsterdam 1987
8. Goodenough  
Psychophysical Perception of Computed Tomography Images  
In: Newton and Potts (eds). Radiology of the skull and brain: technical aspects of  
computed tomography. Vol 5, St. Louis: CV Mosby, 1981:3993-4021
9. Goodenough and Atkins  
Theoretical and Practical Aspects of Automated Quality Assurance Approaches,  
Particularly for CT  
Proceedings of the ICR 89, Excerpta Medica Press, Amsterdam 1990
10. Goodenough, Levy, and Kasales  
Development of Phantoms for Spiral CT  
Comput. Medical Imaging and Graphics 22 (1998) 247-255
11. Goodenough and Weaver  
Factors Related to Low Contrast Resolution in CT Scanners  
Computerized Radiology Vol. 8 No, 5. 279-308 1984

12. Goodenough, Weaver, and Davis  
Development of a Phantom for Evaluation and Assurance of Image Quality in CT Scanning  
The Proceedings of the Application of Optical Instrumentation in Medicine V meeting sponsored by The Society of Photo-Optical Instrumentation Engineers and The Society of Photographic Scientists and Engineers, September 16-19, 1976, Washington DC; and, Optical Engineering, January 1977
13. Goodenough, Weaver, and Davis  
Potential Artifacts Associated with the Scanning Pattern of the EMI Scanner  
Radiology 117:615-620, December 1975
14. Goodenough, Weaver, and Davis  
Physical Measurement of the EMI Imaging System  
In: Ter-Pogossian, Phelps, Brownell, Cos Jr., Davis and Evens (eds). Reconstruction tomography in diagnostic radiology and nuclear medicine. Baltimore: University Park Press, 1977: 225-243
15. John M. Boone and J. Anthony Seibert, 1997, An accurate method for computer-generating tungsten anode x-ray spectra from 30 to 140 kV, Medical Physics, v. 24, No. 11, p. 1661-1670.
16. R. J. Kriz and Keith J. Strauss, 1985, An investigation of computed tomography (CT) linearity, Medical Imaging and Instrumentation, v. 555, p. 195-204.
17. McCullough  
Photon Attenuation in Computed Tomography  
Medical Physics, 2:307-320, Nov/Dec 1975
18. McCullough, Baker, Hattery, Sheedy, Stephens and Payne  
Performance Evaluation and Quality Assurance of Computed Tomography (CT) Equipment with Illustrative Data for ACTA, Delta, and EMI Scanners  
Radiology 120: 173-188, July 1976
19. McCullough, Baker, Houser, and Reese  
An Evaluation of the Quantitative and Radiation Features of Scanning X-ray Transverse Axial Tomography: the EMI Scanner  
Radiology 111: 709-715, June 1974
20. Phelps, Hoffmar-Pogossian  
Attenuation Coefficients of Various Body Tissues, Fluids and Lesions at Photon Energies of 18 to 136 keV  
Radiology 117:573-583, December 1975
21. Rossmann  
Point Spread Function, Line Spread Function and Modulation Transfer Function: Tools for the Study of Imaging Systems  
Radiology 1969:93:257-72
22. T. R. Fewell, R. E. Shuping, and K. E. Healy, 1981, Handbook of Computed Tomography X-ray Spectra, HHS Publication (FDA) 81-8162 (U.S. Government Printing Office, Washington D.C.).
23. Weaver, Goodenough, and Briefel  
Sensitometry in Computerized Tomography  
Proceedings of SPIE, Medicine VI. 1977:127:87-94

24. Yester and Barnes  
Geometrical Limitations of Computed Tomography (CT) Scanner Resolution  
Optical instrumentation in Medicine VI. SPIE, 1977:127:296-303

